Kinks and conformational defects in nonlinear chains

Fei Zhang and Michael A. Collins
Research School of Chemistry, Australian National University, Canberra, Australian Capital Territory 0200, Australia

Yuri S. Kivshar
Optical Sciences Centre, Australian National University, Canberra, Australian Capital Territory 0200, Australia

(Received 14 November 1994)

We introduce a type of nonlinear model, in which the nearest-neighbor interactions have *multiple* local minima, to describe *simultaneously* topological solitons (kinks) and localized static *conformational defects*. We analyze the dynamics of the kinks, including kink-defect interactions. By numerical simulations and a collective-coordinate analysis, we find that the kink propagation can be strongly modified due to the presence of the conformational defects.

PACS number(s): 03.40.Kf, 63.20.Ry, 61.71.Bb, 63.20.Pw

The dynamics of topological solitons in many solids can be described by the well known Frenkel and Kontorova (FK) model (see the review article [1]), which has been used to study many physical phenomena including charge density waves in quasi-one-dimensional conductors, commensurate-incommensurate phase transitions, and domain walls in magnetic and ferroelectric systems, to cite just a few [1—7]. In its simplest version, the FK model describes a chain of particles (atoms) interacting via harmonic forces and subject to a sinusoidal substrate potential. Recently, several important generalizations of this model have been proposed to describe more realistic physical situations, e.g., nonconvex interparticle interactions [4–8].

Chain twisting in polymer crystals has been previously modeled with the FK-type models [9–13], *without* including very important types of physical excitations, which are associated with torsional disorder such as $-tgtg't-$ defects in polymer crystals [13,14]. These conformational defects play a very important role in the premelting phase of the crystals as they are quite populous due to their low conformational energy. Furthermore, kinks themselves may be created more easily in the vicinity of conformational defects; this mechanism of defect-assisted kink creation was suggested by Boyd and Sayre [15] on the basis of dielectric relaxation experiments on polyethylene (PE) crystals.

The main objective of the present paper is to introduce a type of nonlinear lattice model to describe not only kinks but also conformational defects. We consider the dynamics of a discrete system characterized by rotational degrees of freedom ϕ_n. The nearest-neighbor interaction in the chain is described by the potential, $W(\phi_{n+1}-\phi_n)$, which should be periodic in the relative displacement $x \equiv \phi_{n+1}-\phi_n$. To include conformational defects in our model we assume that the periodic potential $W(x)$ has *multiple local minima*, and that it is approximated by

$$W(x) = K[1-\alpha\cos(x)-\beta\cos(3x)], \tag{1}$$

α and β being positive, $\alpha+\beta=1$, and $\alpha \ll \beta$. As shown in Fig. 1, the function $W(x)$ has a global minimum at $x=0$, corresponding to the ground state (GS), and two local minima at $x \approx \pm\frac{2\pi}{3}$, corresponding to metastable states (MS). The energy difference between the GS and the MS is $\Delta E = \frac{3}{2}\alpha K$.

Similar to the conventional FK model, the on-site (substrate) potential, which is responsible for the existence of topological kinks, is taken as

$$U(\phi) = U_0[1-\cos(p\phi)], \tag{2}$$

$p = 1, 2, \ldots$ being an integer.

The equations of motion for the discrete chain may be written in the standard form,

$$I\ddot{\phi}_n - [W'(\phi_{n+1}-\phi_n) - W'(\phi_n-\phi_{n-1})] + U'(\phi_n) = 0. \tag{3}$$

where the parameter I characterizes the inertia of rotation. As has been mentioned above, the chain model (1)–(3) can be used as an alternative phenomenological description of the *twisting* motions of a long polymer chain in crystals. In this context, the dynamical variables ϕ_n represent the setting angles of polymer units. The nearest-neighbor interaction in such a chain is mainly due to the torsional energy of the polymer backbone [13], so it is naturally periodic and has multiple local minima. The substrate potential $U(\phi)$ models the effective force field due to the whole crystal environment [9–14].

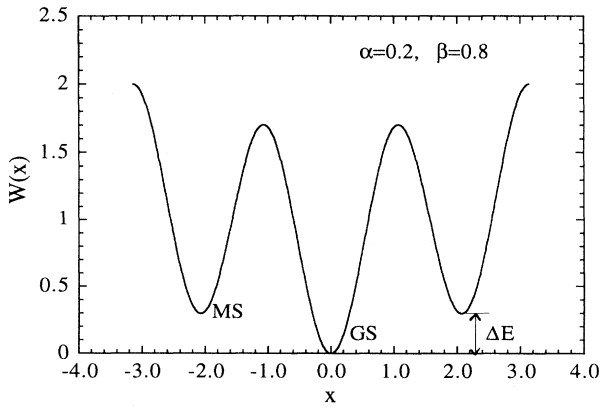

FIG. 1. Structure of the nearest-neighbor interaction potential.

For the sake of simplicity, we use dimensionless units below, assuming $I = K = 1$. In the continuum approximation, valid when ϕ_n changes slowly with n on the scale of the lattice spacing (equal to unity), we have $\phi_{n+1} - \phi_n \approx \phi_x$, and Eq. (3) is reduced to

$$\phi_{tt} - W''(\phi_x)\phi_{xx} + U'(\phi) = 0, \tag{4}$$

where $W''(\phi_x) = \alpha\cos(\phi_x) + 9\beta\cos(3\phi_x)$. Assuming that Eq. (4) has traveling wave solutions of the form $\phi(x,t) = \phi(x - Vt) \equiv \phi(z)$, we have

$$V^2\phi_{zz} - [\alpha\cos(\phi_z) + 9\beta\cos(3\phi_z)]\phi_{zz} + pU_0\sin(p\phi) = 0. \tag{5}$$

From the first integral of Eq. (5), we can show that kinks exist if and only if the following condition holds (see Refs. [5,8]):

$$\bar{F}(V) = \max_{\phi_z}\{F(\phi_z, V)\} \geq 2U_0, \tag{6}$$

where

$$F(\phi_z, V) = -\frac{1}{2}V^2\phi_z^2 + \alpha\phi_z\sin(\phi_z) + 3\beta\phi_z\sin(3\phi_z) + \alpha[\cos(\phi_z) - 1] + \beta[\cos(3\phi_z) - 1]. \tag{7}$$

Expanding $F(\phi_z, V)$ into Taylor series in ϕ_z we find from (6) and (7) the (approximate) critical velocity:

$$V_{\rm cr} \approx \sqrt{\alpha + 9\beta - \sqrt{4U_0(\alpha + 81\beta)}}. \tag{8}$$

Apparently, this critical velocity is smaller than the phonon velocity, $V_{\rm ph} = \sqrt{\alpha + 9\beta}$. Setting $V_{\rm cr} = 0$ in Eq. (8) gives a critical value for the parameter U_0, $U_{\rm cr} = \frac{(\alpha+9\beta)^2}{4(\alpha+81\beta)}$. If the height of the substrate potential is larger than $2U_{\rm cr}$, there will be no smooth kinks in the system.

Given the complexity of the nearest-neighbor interaction, it seems impossible to obtain exact analytical kink solutions for Eq. (5) even though its first integral is available. However, reasonably accurate solutions can be calculated by a perturbation method or variational approach [8]. Here in the case that the substrate potential (2) is much weaker than the nearest-neighbor interaction (1), it is appropriate to assume that $\phi(x)$ varies slowly ($|\phi_x| \ll 1$), so that $W''(\phi_x) \approx W''|_{\phi_x=0} = (\alpha + 9\beta) \equiv \bar{K}$; then Eq. (5) can be approximated by the well known (static) sine-Gordon (SG) equation, $(V^2 - \bar{K})\phi_{zz} + pU_0\sin(p\phi) = 0$. Therefore the kink (antikink) solution of Eq. (4) may be approximated by

$$\phi_k(x,t) = \frac{4}{p}\tan^{-1}\left\{\exp\left[\pm\frac{p[x - X(t)]}{\sqrt{(\bar{K} - V^2)/U_0}}\right]\right\}, \tag{9}$$

where $X(t) = Vt + x_0$, V being the kink's velocity. In fact, it is easy to verify that $|d\phi_k(x,t)/dx| \leq 2\sqrt{U_0/(\bar{K} - V^2)} \ll 1$, if $U_0 \ll \bar{K} - V$. Using the approximate analytical solution (9), the energy of a static kink is estimated as

$$E_s = \int_{-\infty}^{\infty}\{\tfrac{1}{2}\bar{K}\phi_x^2 + U_0[1 - \cos(p\phi)]\}dx = 8\sqrt{U_0\bar{K}}/p. \tag{10}$$

The analytical solutions (9) can be considered as an approximate kink solution of (3), and it also can be used as an initial condition in numerical calculations to find more accurate kink solutions of the discrete system. We found that Eq. (9) can provide a fairly good approximation to the kink solution of Eq. (3) [see Fig. 2(a)]. For example, at $\alpha = 0.3, \beta = 0.7, U_0 = 0.1$, and $p = 1$, Eq. (10) gives $E_s = 6.499$, while the numerical calculation yields $E_s = 6.396$.

In addition to the kinks, many types of localized static solutions exist in the *discrete* system (3) ($\ddot{\phi}_n = 0$, for all n). Such static defects appear due to the existence of the deep local minima (metastable states) in the potential $W(x)$. Figure 2(b) shows one of the *simplest* defect located at the site $m = 100$. This defect can be approximated as $\phi_n = \sigma\frac{2\pi}{3}\delta_{m,n}$, $n = 1, 2, ...$, where $\delta_{m,n} = 1$ for $n = m$, and $\delta_{m,n} = 0$ for $n \neq m$. The sign function $\sigma = +1$ or $\sigma = -1$ represents two types of defects denoted by D^+ and D^-, respectively. The energy of such a defect can be estimated to be $E_d = 2\Delta E = 3\alpha$, and at $\alpha = 0.3, \beta = 0.7, U_0 = 0.1$, and $p = 1$ the analytical and numerical results are 0.9 and 1.032, respectively. Note that the system (3) supports many other types of conformational defects, which might be viewed as super-

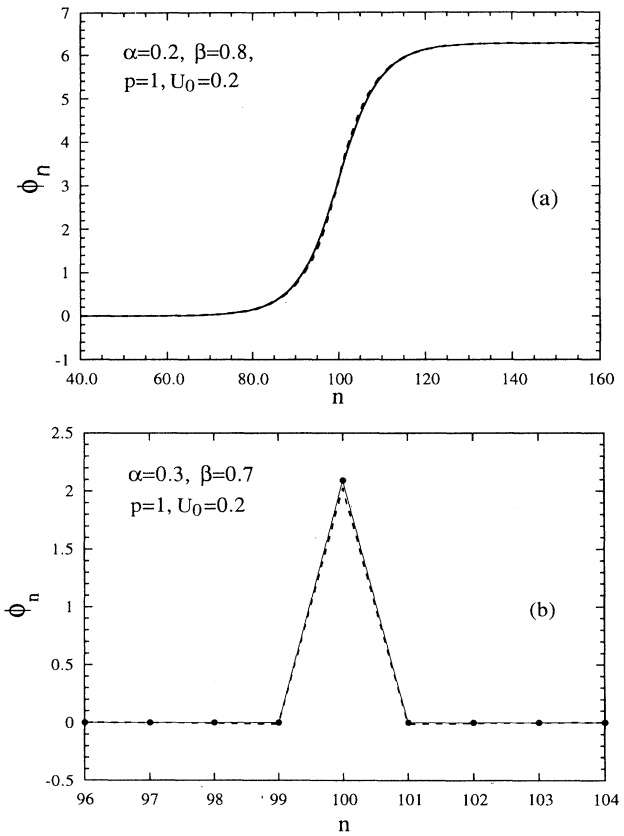

FIG. 2. (a) Static kink solution obtained by numerical simulations with damping (dashed curve), compared with the analytical approximation (9). (b) Shape of the conformation defect calculated numerically (dashed curve), compared with the simple analytical approximation (solid curve with filled circles).

positions of the simplest defects shown in Fig. 2(b).

Once the basic nonlinear modes have been obtained, it is useful to investigate their dynamical properties. First, we have found in numerical simulations that the kinks can propagate smoothly at low velocities [cf., Eq. (8)]. However, high velocity kinks are unstable and they may be broken into very sharply varying waveforms and become pinned, as expected from the above analysis. The sharp kinks may contain one or two overtwisted angles, i.e., $\phi_{k+1} - \phi_k \approx 2\pi/3$. Second, equal-velocity and head-on collisions of kink and antikink are examined to be inelastic: above a threshold velocity the kinks may pass through each other and escape to infinity, while below the threshold velocity the kinks may be trapped together and form a *breather* excitation. This phenomenon is typical for nonintegrable FK-type models.

Third, the propagation of a kink will also be influenced by the conformational defects in the chain. Here we consider the interactions of a kink with the simplest type of defect that is shown in Fig. 2(b). To understand the nature of such interactions, we use a collective-coordinate approach (see, e.g., [16,17]), which replaces the infinitely many degrees of freedom of the system by a number of physically important variables. Such a reduction is usually helpful for one to extract the main physical effects that might appear in a complex nonlinear system. In particular, to study the kink dynamics under perturbations, it is essential to select the position of the kink's center as a collective coordinate [17]. So here we use the following ansatz:

$$\phi(n, X(t)) = \phi_k(n, X) + \frac{2\pi}{3}\delta_{m,n} \quad , \tag{11}$$

where $\phi_k(n, X)$ is defined by Eq. (9), and the kink's center X is considered as a collective variable. Inserting this ansatz into the system Lagrangian, and neglecting a constant term of kink energy and a very small Peierls-Nabarro potential (due to discreteness effects on the kink), in the lowest order approximation we obtain the following effective Lagrangian:

$$L_{\text{eff}} = \frac{1}{2}M_s\dot{X}^2 - \bar{U}(X), \tag{12}$$

where the first term is the kinetic energy of the kink, M_s being the kink's mass, and the second term is the effective interaction potential between the kink and defect,

$$\begin{aligned}\bar{U}(X) = U_0\{&\cos[p\phi_k(m, X)] - \cos[p\phi_k(m, X) + 2p\pi/3]\} \\ &+W\left[\Delta\phi_k(m) + \frac{2\pi}{3}\right] - W[\Delta\phi_k(m)] \\ &+W\left[\Delta\phi_k(m+1) - \frac{2\pi}{3}\right] - W[\Delta\phi_k(m+1)]\end{aligned} \tag{13}$$

where $\Delta\phi_k(m+1) \equiv \phi_k(m+1, X) - \phi_k(m, X)$. As shown in Fig. 3, the potential $\bar{U}(X)$ is *attractive* and slightly *asymmetric*. Some results about the kink-defect interactions can thus be anticipated from the collective-coordinate approach. During the kink-defect interac-

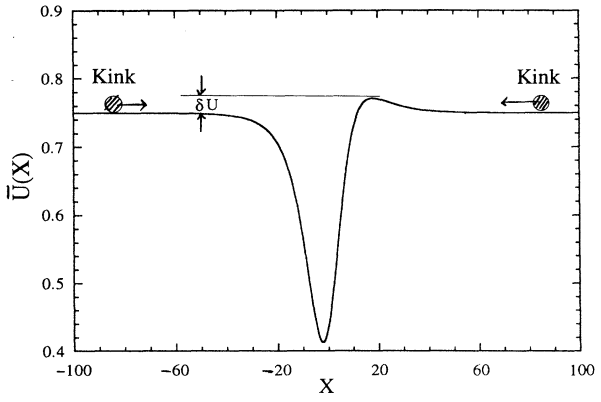

FIG. 3. Effective potential $\bar{U}(x)$ for the kink, created by a conformational defect located at $m = 0$. Model parameters are $\alpha = 0.2, \beta = 0.8, U_0 = 0.1$, and $p = 1$. Here $\delta U \approx 0.021$ is the difference between the maximum and asymptotic value of the potential.

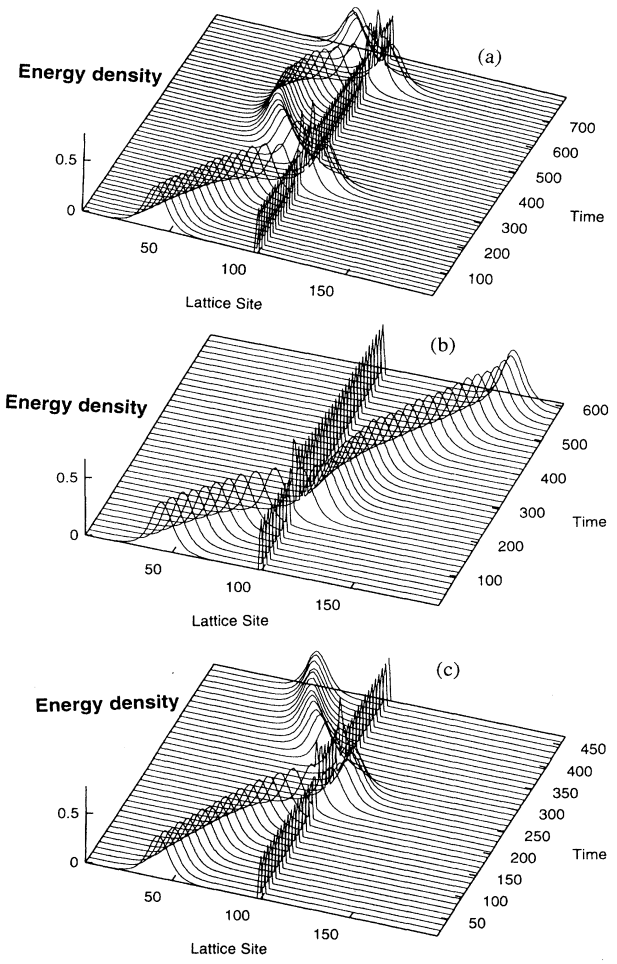

FIG. 4. Kink-defect interactions at $\alpha = 0.2$, $\beta = 0.8$, $U_0 = 0.1$, $p = 1$, for different values of the kink's initial velocity V: (a) Trapping, $V = 0.15$; (b) Passing, $V = 0.28$; (c) Reflection, $V = 0.2$. The final kink's velocity in this case is $V_f = -0.117$.

tions, part of the kink's kinetic energy will be lost due to radiation of small amplitude phonon waves, thus a low-velocity kink may be *trapped* in the potential well created by the defect, while a high-velocity kink will be able to *pass* the defect with a reduced final velocity. If the kink comes to the defect from the left [see Figs. 3 and 4(a)], the kink may be *reflected* by the defect if its initial velocity is in a small interval which depends on the potential barrier δU. Consider the kink as a classical particle and suppose that its kinetic energy after collision is $\delta E_k = \frac{1}{2}M_s V_i^2 - \frac{1}{2}M_s V_{c1}^2$, where V_i is the kink's initial velocity, and V_{c1} is the critical velocity below which the kink will be trapped by the defect. Then the condition for the kink to be reflected is $\delta E_k \leq \delta U$, from which we find the critical value for V_i: $V_{c2} = \sqrt{V_{c1}^2 + 2\delta U/M_s} > V_{c1}$. Therefore, if the kink's velocity is in the interval (V_{c1}, V_{c2}), the kink will be reflected.

To examine the validity of the physical picture derived from the collective-coordinate analysis, we have simulated the kink-defect interactions numerically taking the paramters $\alpha = 0.2, \beta = 0.8, U_0 = 0.1$, and $p = 1$. The results are summarized as follows. If the kink's velocity is smaller than $V_{\rm cr} = 0.16$, the kink will be trapped by the defect [Fig. 4(a)]; if the kink's initial velocity is larger than 0.265, it will pass the defect. Figure 4(b) shows that after the transimision of the kink, the defect remains unchanged (which means that the defect is rather stable). In the velocity interval (0.16, 0.265) we observe that the kink is reflected by the defect and escapes in the *opposite* direction [Fig. 4(c)]. These results agree qualitatively with the collective-coordinates analysis.

Since the effective potential is asymmetric, the results of kink-defect interactions in which the kink comes from the other direction (see Fig. 3) are different from those that have just been described. The incoming kink first experiences a repulsive potential which attains a maximum at about 18 sites away from the defect. Therefore, at very lower velocity the kink will be reflected by the repulsive potential; and at slightly higher velocity, a kink will be able to overcome the barrier to interact with the defect.

It is worth comparing the kink-defect interactions studied here with the kink-impurity interactions analyzed in [17]. The major difference is that the static conformational defect here supports no localized oscillating mode. However, from the linear spectrum analysis around the kink we have found that the kinks in our model possess an oscillating "internal mode" (similar to the case of the ϕ^4 model) at least for some ranges of the model parameters α, β, U_0. Thus, according to the theory developed in [17], the kink internal mode might play a special role, including resonances in the kink-defect interactions. However, the resonance phenomena, if they exist, are likely to be very sensitive to perturbations of initial kink profile, while exact analytical kink solutions in the present discrete chain are not available, and discreteness effects will not be negligible when $U_0 \geq 0.2$.

In conclusion, we have presented a nonlinear chain model to describe simultaneously kinks and conformational defects. We have shown that kinks can propagate freely in the chain provided their velocity does not exceed a threshold value due to the anharmonicity of the interparticle interactions. However, the kink's motion can be strongly affected by the conformational defects, which create an asymmetric attractive potential to the kink. Trapping, passing, and reflection of the kink are predicted in terms of a collective-coordinate approach, and are observed in numerical simulations. Our model can be used to describe smooth kinks and conformational defects on long polymer chains, where the dynamics of the kinks might be significantly influenced by conformational defects (torsional disorder) as previously suggested [18].

[1] W. Selke, in *Phase Transitions and Critical Phenomena*, edited by C. Domb and J.L. Lebowitz (Academic, New York, 1992), Vol. 15.

[2] V.G. Baryakhtar, B.A. Ivanov, and A.L. Sukstanskii, Zh. Eksp. Teor. Fiz. **78**, 1509 (1980) [Sov. Phys. JETP **51**, 757 (1980)].

[3] P. Bak, Rep. Prog. Phys. **45**, 587 (1982).

[4] S. Aubry, Physica D **7**, 240 (1983); S. Aubry and P.Y. Le Daeron, *ibid.* **8**, 381 (1983).

[5] A. Milchev, Phys. Rev. B **42**, 6727 (1990); Physica D **41**, 262 (1990).

[6] I. Markov, Phys. Rev. B **48**, 14 016 (1993).

[7] K.E. Bassler and R.B. Griffiths, Phys. Rev. B **49**, 904 (1994).

[8] O.M. Braun, F. Zhang, Yu.S. Kivshar, and L. Vazquez, Phys. Lett. A **157**, 241 (1991).

[9] H. Dvey-Aharon, T.J. Sluckin, P.L. Taylor, and A.J. Hopfinger, Phys. Rev. B **21**, 3770 (1980).

[10] M.L. Mansfield, Chem. Phys. Lett. **69**, 383 (1980).

[11] J. L. Skinner and P.G. Wolynes, J. Chem. Phys. **73**, 4015 (1980); J.L. Skinner and Y.H. Park, Macromolecules **17**, 1735 (1984).

[12] K. Fukao, J. Chem. Phys. **92**, 6867 (1990).

[13] F. Zhang and M.A. Collins, Phys. Rev E **49**, 5807 (1994); Chem. Phys. Lett. **214**, 459 (1993).

[14] D.C. Doherty and A.J. Hopfinger, Phys. Rev. Lett. **72**, 661 (1994).

[15] R.H. Boyd and J.A. Sayre, J. Polym. Sci: Polym. Phys. **17**, 1627 (1980).

[16] R. Ravelo, M. El-Batanouny, C.R. Willis, and P. Sodano, Phys. Rev. B **38**, 4817 (1988); C.R. Willis and R. Boesch, *ibid.* **41**, 4570 (1990).

[17] F. Zhang, Yu.S. Kivshar, and L. Vazquez, Phys. Rev. Lett. **67**, 1177 (1991); Phys. Rev. A **45**, 6019 (1992); **46**, 5214 (1992).

[18] M.D. Zoppo and G. Zerbi, Polymer **33**, 4667 (1992).